UNIVERSITY OF BIRMINGHAM

Research at Birmingham

Vapour–liquid equilibrium of propanoic acid+water at 423.2, 453.2 and 483.2K from 1.87 to 19.38bar. Experimental and modelling with PR, CPA, PC-SAFT and PCP-SAFT

Roman Ramirez, Luis; García-sánchez, Fernando; Santos, Regina; Leeke, Gary

Link to publication on Research at Birmingham portal

Accepted Manuscript

Title: Vapour–Liquid Equilibrium of Propanoic Acid + Water at 423.2, 453.2 and 483.2 K from 1.87 to 19.38 bar. Experimental and Modelling with PR, CPA, PC-SAFT and PCP-SAFT
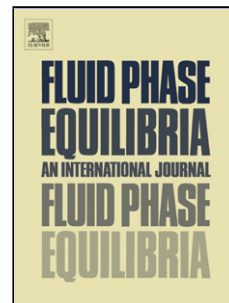
Author: Luis A. Román-Ramírez Fernando García-Sánchez Regina C.D. Santos Gary A. Leeke

Please cite this article as: Luis A.Román-Ramírez, Fernando García-Sánchez, Regina C.D.Santos, Gary A.Leeke, VapourndashLiquid Equilibrium of Propanoic Acid + Water at 423.2, 453.2 and 483.2K from 1.87 to 19.38bar.Experimental and Modelling with PR, CPA, PC-SAFT and PCP-SAFT, Fluid Phase Equilibria http://dx.doi.org/10.1016/j.fluid.2015.01.004

This is a PDF file of an unedited manuscript that has been accepted for publication. As a service to our customers we are providing this early version of the manuscript. The manuscript will undergo copyediting, typesetting, and review of the resulting proof before it is published in its final form. Please note that during the production process errors may be discovered which could affect the content, and all legal disclaimers that apply to the journal pertain.

Vapour – Liquid Equilibrium of Propanoic Acid + Water at 423.2, 453.2 and 483.2 K from 1.87 to 19.38 bar. Experimental and Modelling with PR, CPA, PC-SAFT and PCP-SAFT

Luis A. Román-Ramírez [a,*], Fernando García-Sánchez [b], Regina C.D. Santos [a], Gary A. Leeke [a]

[a] School of Chemical Engineering, University of Birmingham, Edgbaston, Birmingham B15 2TT, United Kingdom.

[b] Laboratorio de Termodinámica, Programa de Investigación en Ingeniería Molecular, Instituto Mexicano del Petróleo. Eje Central Lázaro Cárdenas 152, 07730 México, D.F., México.

[*] Corresponding author. Tel.: (+44) 0121 414 6965. E-mail address: LAR058@bham.ac.uk.

Graphical abstract

Abstract

Vapour – liquid equilibrium data were measured for the propanoic acid + water system at 423.2, 453.2 and 483.2 K from 1.87 to 19.38 bar over the entire range of concentrations. An experimental apparatus based on the static-analytical method with sampling of both phases was used with quantitative analysis by GC. The system is highly non-ideal showing azeotropic behaviour. The Peng-Robinson (PR), the Cubic Plus Association (CPA), the Perturbed Chain Statistical Associating Fluid Theory (PC-SAFT) and the PC-Polar-SAFT (PCP-SAFT) equations of state modelled the data. Two association sites were assumed for both compounds. A single-binary interaction parameter (k_{ij}) was used in all models, and predictive ($k_{ij} \quad 0$) and correlative ($k_{ij} \quad k_{ij}^{0} \quad k_{ij}^{1}T$) capabilities were assessed. Available data at 313.1, 343.2 and 373.1 K from the open literature were included in the analysis. PCP-SAFT presented higher predictive and correlative

capabilities over the entire temperature range. PC-SAFT in predictive mode was not able to represent the azeotropic behaviour but resulted in the second best correlations. CPA presented a satisfactory balance between the two modes. PR predictions were rather poor but correlations were better than those of CPA, at the expense of a larger k_{ij}.

Keywords:

propanoic acid; water; vapour liquid equilibrium; PC-SAFT; CPA; PR Introduction

Propanoic acid market value is estimated to reach 1,622.2 million USD by 2018, mainly driven by its application as a food preservative which account for nearly 78% of the global consumption [1]. Other major applications include polymer synthesis, pharmaceuticals and solvents formulation [2]. It is industrially produced by three main routes: ethylene carbonylation, oxidation of propanal and direct oxidation of hydrocarbons [2,3]. Regardless of the process, desired purity is usually achieved by removing water and other acids through distillation. Propanoic acid also appears as one of the many degradation products from the hydrothermal treatment of biomass [4,5]. Experimental data are thus needed at a wide range of temperature and pressure conditions, and additionally a reliable thermodynamic model for correlation or predictive purposes. Work currently found in the literature report data only at low temperatures or near atmospheric pressures.

Earlier research on the vapour – liquid equilibria (VLE) of propanoic acid + water systems dates back to 1942 with Giacalone et al. [6] who reported bubble point pressures at 307.58 K and showed what seems to be an azeotrope in the 0.01 – 0.03 propanoic acid mole fraction region. A year later, Othmer [7] reported azeotropic behaviour at 1 bar near 373 K. Ghmeling and Onken [8] compiled most of the subsequent work, which were largely sub- and atmospheric measurements up to 414.53 K. More recent articles by Miyamoto et al. [9] and Olson et al. [10], reported data at 343.2 K

and liquid compositions at or below atmospheric pressure, respectively. Azeotropic behaviour has been reported in most of these studies.

Modelling with Equations of State (EoS) is preferred over correlations or activity coefficient models since all thermodynamic properties can be obtained from the same equation. In the present work, the Peng Robinson (PR), the Cubic Plus Association (CPA) and the Perturbed Chain Statistical Associating Fluid Theory (PC-SAFT) were chosen with the aim to determine the most suitable model for the propanoic acid + water system.

PR is an empirical cubic equation and was selected for its simplicity and widespread industrial application; it has been reliable in modelling mixtures varying in nature and complexity [11,12]. PC-SAFT belongs to a group of theoretical EoS of the SAFT family which accounts for different intermolecular interactions explicitly and has been applied successfully in modelling properties of simple and complex mixtures, including polymer systems [13]. CPA can be considered an intermediate EoS between these two groups. Developed by coupling a cubic equation with an association term, it retains most of the simplicity of an empirical model but with increased accuracy [14].

In SAFT-type EoS such as PC-SAFT and CPA, the type of association bonding has to be established for the compounds involved. For this purpose, the classification of Huang and Radosz [15] is commonly used as a guidance (Figure 1). Water, for instance, is rigorously modelled as having four association sites (4C): two lone-pairs of electrons and two hydrogen atoms; whereas carboxylic acids are modelled as having one association site (1A) which are able to bond with a similar site. Although the 4C rigorous type for water is more in line with experimental spectroscopy data [14,16,17], there is no general agreement on the best association model especially when applied to real mixtures. A 3B and even a 2B assignment could be justified and has led to satisfactory results [18-22]. Furthermore, different sets of parameters of the

same association scheme may result in different outcomes in the modelling of pure compounds and/or mixtures properties, demonstrated in the comparisons of Kleiner [19], von Solms et al. [16] and recently by Liang et al. [22].

It is now generally accepted that carboxylic acids have a tendency to form cyclic dimers in the vapour phase and linear chains in the solid phase, however there is still no universal consensus about the predominant form in the liquid phase. New investigations show that the main structure in the liquid phase may also be cyclic dimers, rather than linear chains as was previously suggested [23]. Dimerization is caused by the formation of two hydrogen bonds between the carboxylic groups of two acid molecules. This can be captured by applying the rigorous 1A association type, in which only cyclic dimers are allowed to form. However, the fact that chain-monomers may appear in the liquid phase also allows for a 2B association model.

Kleiner [19] and Kleiner et al. [24] have shown for PC-SAFT the 1A scheme represents better pure compound properties compared with the 2B association scheme for organic acids (from formic acid to decanoic acid). Derawi et al. [25] arrived at the same conclusion for CPA when testing types 1A, 2B and even 4C in predicting vapour pressures and equilibrium constants of formic, acetic and propanoic acids. More recently, Janecek and Paricaud [26] have tested the 1A, 2B and the doubly bonded dimer (DBD) scheme of Sear and Jackson [27,28] in the modelling of the formic acid to pentanoic acid series with PC-SAFT; the reported deviations for the saturated properties of the 1A and 2B schemes did not reveal a preferred choice.

In respect to the modelling of organic acid + water mixtures with PC-SAFT, it is pertinent to mention the studies of Kouskoumvekaki et al. [29] and Chen et al. [21], who defined both compounds as 2B; and the studies of Janecek and Paricaud [30] who compared the cases for acetic acid and propanoic acid modelled either as 2B or DBD and water as 4C (the 2B type was also investigated for the case with acetic acid). Predictions with water modelled as 2B were superior to

the 4C cases, but the latter showed improved correlations. On the other hand, slightly better predictions and correlations were achieved by the DBD scheme.

Kontogeorgis et al. [31] modelled with CPA the propanoic acid + water system at 1 atm defining the acid as 1A and water as 4C. Although a large negative binary interaction parameter was needed, CPA satisfactorily fitted the experimental data. In contrast, Kontogeorgis and Folas [14] have reported that better results could be obtained by considering acetic acid as 2B in the acetic acid + water mixture. In order to improve the capabilities of CPA, particularly for the acetic acid + water system, Muro-Suñé et al. [32] modified CPA by introducing the Huron-Vidal mixing rule with a modified non-random two-liquid expression (NRTL).

Propanoic acid and water are both dipolar compounds. It is therefore appealing to model this system by considering the association and polar terms explicitly in the PC-SAFT Helmholtz expansion. This approach, however, might not necessarily be in agreement with the actual phenomenon since both interactions are not independent of one another [20,33]. It may in some cases improve the fitting as found for CO_2 + alkanol mixtures [34,35] or it could also lead to worse results, as shown for the acetone + water system [36]. To our knowledge, only the work of Soo [19] has included polar contributions for the modelling of organic acids, but no comparison against the non-polar version was done. Expressions for induced dipolar contributions have also been proposed within the PC-SAFT framework [13] but are not studied here.

In the present work, phase equilibria data for propanoic acid + water were generated and modelled with the selected EoS. Comparisons of predictive and correlative performance were made. Self- and cross-association interactions were modelled assuming a 2B scheme [15] for both compounds, for simplicity, and because it is the association scheme more readily available in commercial simulation software. Additionally, the case with polar contributions in PC-SAFT was also

studied with the aim to determine the effect of including both terms simultaneously in the Helmholtz expansion. Pure component parameters were refitted in each case.

1. Experimental Section

1.1 Materials

Propanoic acid and water were ACS reagent grade from Sigma-Aldrich; no further purifications were performed. Propanoic acid purity was checked by gas-chromatography (GC) and determined to be 0.9798 mole fraction. The impurity was identified to be mostly water, in agreement with its hydrophilic characteristics. Helium carrier gas for GC analysis was obtained from BOC with a certified purity ≥ 99.999%.

1.2 Experimental Apparatus and Uncertainties

An apparatus based on the static-analytical method with sampling of a vapour and a liquid phase was used for the measurements. A modified high-pressure vessel (Parr 4575 series) made of Hastelloy C to resist corrosive attack [37] served as the equilibrium cell. It had a nominal volume of 250 mL with wall thickness of approximately 17 mm. Two SS-316 dip tubes (20 cm length for the liquid and 5 cm for the vapour phase) internal diameter (ID) 0.004" were used to sample the phases via two 1/16" ball valves (Swagelok). PEEK tubing, 3 cm length, 0.064 mm ID, was used downstream immediately after the valves. Internal diameters and lengths were chosen to minimize dead volume. A pressure digital gauge (Keller-Druck, model Lex1), range 0 – 20 bar, measured pressure with a ±0.01 bar accuracy according to manufacturer's calibration certificate. Combined standard uncertainties in pressure, $u_c(P)$, after considering calibration, repeatability and pressure drop during sampling were $u_c(P)$ = 0.01 bar.

An oven (Applied Separations, model Spe-ed SFC) previously used for supercritical extractions was modified to act as the temperature control environment. Temperature was controlled to within 0.1 K. A thermocouple data logger (Pico Technology, model TC-08) monitored and recorded temperature. A T-type thermocouple inside a thermowell measured temperature at the interior of the equilibrium cell. Three other thermocouples, one at the side, one at the outside bottom of the equilibrium cell and one at the middle of the oven gave a temperature profile. Thermocouples were calibrated by comparing measured saturated temperatures of water from 301 to 487 K against equilibrium data from NIST [38]. Combined standard uncertainties in temperature, $u_c(T)$, after calibration, control and resolution are $u_c(T)$ = 0.1 K.

A vacuum pump (KNF Neuberger Edwards, model Laboport PM 13196-840.3) vacuumed the cell at the beginning of each experiment. Water was loaded into the cell by means of a digital high pressure pump (Jasco, model PU-1586). A Hastelloy C internal stirrer attached to a magnetic drive in the cell head agitated the mixture to induce equilibrium. A schematic diagram of the apparatus is shown in Figure 2.

Quantitative analysis was done by GC (Agilent Technologies, model 6850) equipped with TCD detector and a packed column 3 ft x 1/8 in SS Porapak N 80/100 mesh (Speck & Burke Analytical). 0.2 μL sample volumes were injected with an autosampler for precision and reproducibility. A GC calibration curve was prepared by injecting mixtures of known propanoic acid + water composition. A linear relationship of area ratio vs. mass fraction ratio was obtained from the low to the high propanoic acid concentration regions. Uncertainties in composition for each experimental point are shown in the corresponding results table (Table 1).

1.3 Procedure

Before each experimental run, the equilibrium cell was washed and rinsed with ethanol and left to dry in an oven. It was then allowed to reach room temperature and a pressure test with compressed nitrogen carried out. Propanoic acid and water were degassed in an ultrasonic bath (Grant XB6 degasser) for 1 hour. A mixture of propanoic acid and water was immediately loaded into the equilibrium cell and the system vacuumed down to 0.015 – 0.02 bar at room temperature. Desired cell temperature was reached by increasing or decreasing the air bath temperature. The system was allowed to reach equilibrium condition under constant stirring, which was assumed when temperature and pressure did not vary within ±0.05 K and ±0.005 bar, respectively for at least 5 minutes. A minimum of five samples of each phase (20 µL volume each), were withdrawn and collected in 250 µL vial inserts (Agilent Technologies) for further analysis by GC. Sampling was done quick enough to reduce equilibrium perturbation, which was monitored by checking for pressure drops. The maximum pressure drop observed was 0.01 bar. Pressure was then increased by pumping additional water into the cell and a new equilibrium point was then established. Several experiments with different initial overall loadings were needed to complete the full phase diagram.

2. Thermodynamic Modelling

2.1 Peng-Robinson

The Peng-Robinson [39] EoS in terms of the residual Helmholtz free energy ($\hat{a}^{res}$) is [40]:

$$\frac{\hat{a}^{res}}{RT} = \frac{\hat{a}^{PR}}{RT} = \ln\left(1-\frac{b}{v}\right) - \frac{a(T)}{2RTb\sqrt{2}}\ln\left(\frac{1+\left(1+\sqrt{2}\right)\frac{b}{v}}{1+\left(1-\sqrt{2}\right)\frac{b}{v}}\right) \quad (1)$$

where R is the gas constant, T is the temperature, v is the volume and a and b are characteristic parameters of the equation. Critical temperature (Tc), critical pressure (Pc) and acentric factor ( ) properties characterize a component. In this work van der Waals one-fluid mixing rules (Equations 2 and 3) and classical combining rules (Equations 4 and 5) were applied for modelling the mixtures.

$$a = \sum_i\sum_j x_i x_j a_{ij} \quad (2)$$

$$b = \sum_i x_i b_i \quad (3)$$

$$a_{ij} = \sqrt{a_i a_j}(1-k_{ij}) \quad (4)$$

$$b_{ij} = \frac{b_i+b_j}{2} \quad (5)$$

where k_{ij} is the binary interaction parameter.

2.2 CPA

The CPA [41] EoS can be written as:

$$\frac{\hat{a}^{res}}{RT} \quad \frac{\hat{a}^{SRK}}{RT} \quad \frac{\hat{a}^{assoc}}{RT} \tag{6}$$

where $\hat{a}^{SRK}$ and $\hat{a}^{assoc}$ are the Helmholtz free energy contributions given by the Soave-Redlich-Kwong EoS and those of association interactions, respectively. Three parameters are needed to characterize a non-associating compound (a_0, b, c_1) and two additional parameters for an associating compound: energy (^{AB}) and volume (^{AB}) of association. Mixing and combining rules in the SRK contribution are similar to those of Equations (2-5). Cross-association volumes and energies were calculated in this work by the CR1 combining rule [17]:

$$_{A_iB_j} \quad \frac{^{A_iB_i} \quad ^{A_jB_j}}{2} \tag{7}$$

$$_{A_iB_j} \quad \sqrt{^{A_iB_i} \quad ^{A_jB_j}} \tag{8}$$

2.3 PC-SAFT and PCP-SAFT

PC-SAFT can be written as the addition of contributions due to hard-chain fluid formation (*hc*), dispersive (*disp*), association (*assoc*) and *dipolar* forces [13]:

$$\frac{\hat{a}^{res}}{RT} \quad \frac{\hat{a}^{hc}}{RT} \quad \frac{\hat{a}^{disp}}{RT} \quad \frac{\hat{a}^{assoc}}{RT} \quad \frac{\hat{a}^{dipolar}}{RT} \tag{9}$$

Even though several models have been proposed to account for the dipolar contributions in PC-SAFT [13], the one

developed by Gross and Vrabec [42] was adopted in this work since it does not introduce the need of an additional adjustable pure component parameter. Throughout the rest of the manuscript, the model is referred to as PC-polar-SAFT (PCP-SAFT) when the dipolar and the association term are both simultaneously included in the Helmholtz expansion, and simply as PC-SAFT for the non-polar version.

Five pure component parameters are needed to characterize an associating compound, namely, the number of segments per chain (m), the segment diameter ( ), the depth of the pair potential ( ), the association energy (^{AB}) and the association volume (^{AB}). Additionally, the dipole moment ( ) is required in PCP-SAFT; this can be adjusted or taken from experimental data, the latter case is applied here. Details of the physical meaning of the parameters can be found in the original publications [42-44].

The following conventional combining rules for   and   are used for mixtures [43].

$$_{ij} \quad \frac{(\ _i \quad _j)}{2} \tag{10}$$

$$_{ij} \quad \sqrt{\ _i \ _j}(1 \quad k_{ij}) \tag{11}$$

where k_{ij} is introduced to correct the segment-segment interactions of unlike chains.

Combining rules for the cross-association energy and volume are given by Equations (7 and 12), respectively [44]:

$$\epsilon^{A_iB_j} = \sqrt{\epsilon^{A_iB_i} \epsilon^{A_jB_j}} \left(\frac{\sqrt{\sigma_i \sigma_j}}{(\sigma_i + \sigma_j)/2} \right)^3 \tag{12}$$

CPA, PC-SAFT and PCP-SAFT pure compound parameters were obtained by fitting vapour pressure (P_v) and liquid density (ρ_L) data with Equation (13) as the objective function. Multiplicity of optimum parameters in multiparameter-models is well known [34,41]; hence, a simplex algorithm was applied in the optimization since it seems to be less sensitive to the initial guesses [34].

$$OF_1 = \sum_{i=1}^{Np} \left(\frac{P_{V,i}^{exp} - P_{V,i}^{calc}}{P_{V,i}^{exp}} \right)^2 + \left(\frac{\rho_{L,i}^{exp} - \rho_{L,i}^{calc}}{\rho_{L,i}^{exp}} \right)^2 \tag{13}$$

Superscripts *exp* and *calc* stand for an experimental and a calculated property, respectively. *Np* is the number of experimental points used in the optimisation. Average deviations from correlated and experimental saturated properties were calculated according to:

$$\frac{100}{Np} \sum_{i=1}^{Np} \left| \frac{\theta_i^{exp} - \theta_i^{calc}}{\theta_i^{exp}} \right| \tag{14}$$

where θ stands either for P_V or ρ_L.

For all models, a single binary interaction parameter was used. Calculations with $k_{ij} = 0$ and a temperature-dependent k_{ij} were carried out for comparison. The computation algorithm was that of the bubble-point method. The optimum k_{ij} was

obtained by regressing experimental data of bubble point pressures (P) and vapour compositions (y) simultaneously according to the following objective function:

$$OF_2 = \sum_{i=1}^{Np} \left[\left(\frac{P_i^{exp} - P_i^{calc}}{P_i^{exp}} \right)^2 + \left(y_{1,i}^{exp} - y_{1,i}^{calc} \right)^2 \right] \qquad (15)$$

Average deviations between experimental and calculated values were computed according to:

$$\Delta P = \frac{100}{Np} \sum_{i=1}^{Np} \left| \frac{P_i^{exp} - P_i^{calc}}{P_i^{exp}} \right| \qquad (16)$$

$$\Delta y_1 = \frac{1}{Np} \sum_{i=1}^{Np} \left| y_{1,i}^{exp} - y_{1,i}^{calc} \right| \qquad (17)$$

3. Results and Discussion

3.1 Experimental

Vapour - liquid equilibria in the form of *Pxy* data for the propanoic acid + water system were generated at 423.2, 453.2 and 483.2 K from 1.87 to 19.38 bar and are given in Table 1. Relative errors in the measured water vapour pressures against data from NIST are: 0.21, 0.129 and 0.403% at 423.2, 453.2 and 483.2 K, respectively. A positive deviation from ideal behaviour with azeotropism is observed in the low propanoic acid concentration region, below 0.1 mole fraction. A light yellow-greenish colour liquid remained at the end of the experimental runs evidencing corrosion attack primarily to the SS-316 dip tube. A more intense colour was observed at the maximum run temperature of 483.2 K, for which a

0.004% iron content was determined by spectrophotometry. A previous study [45] at more severe conditions showed that a 2% content gave no interference to the phase behaviour.

3.2 Modelling

3.2.1 Pure component parameters

Critical properties and acentric factor of propanoic acid and water are given in Table 2.

The intention of this work was not to find the best set of parameters of CPA, PC-SAFT and PCP-SAFT, and with this in mind only different initial estimates were tested with the aim to locate all local minima. The reported values are those obtained from the testing of several initial guesses that converged to the same minimum value of the objective function (Equation 13).

Pure component parameters of CPA from the optimization are reported in Table 3. Propanoic acid parameters are similar to those previously reported by Derawi et al. [25]. Water parameters differ from those reported for the 2B type by Kontogeorgis et al. [46], but the association energy parameter given in Table 3 is closer to the experimental values [14]. Differences can be attributed to the multiplicity of optimum parameters due to any of the following factors: the temperature range used in the fitting, the source of experimental data and the search algorithm.

In the case of PC-SAFT and PCP-SAFT (Table 3), propanoic acid vapour pressures are slightly better correlated when the dipole moment is considered, with no effect on the liquid densities. Similarly, PCP-SAFT parameters for water result in lower deviations compared with PC-SAFT, for both saturated properties in this case. It is important to note, however, the

unusual values of m (>1) and (<3). Water is almost a spherical molecule and a value of m close to 1 is thus expected; besides, values for are normally higher than 3 Å. Clearly the values reported here do not lie in this range. Nevertheless, values out of this range have been previously reported with satisfactory results (see e.g. [16,47,48]). Arguably, the polar and association interactions taking place might be affecting the shape of the molecule. On the other hand, it is difficult to determine from the values alone, if a set of pure component parameters will result in satisfactory predictions (or correlations) of pure compound and/or mixture properties, as demonstrated in recent investigations [22] of different sets of parameters for water. Determination of the optimum set of parameters is a complex problem and out of the scope of this paper.

3.2.2   Mixtures

In order to test the capabilities of the equations at a wider range of conditions, data at 313.1, 343.2 and 373.1 K available in the open literature [9,49,50] were included in the modelling.

3.2.2.1   *Predictive mode*

The best predictions (k_{ij} 0) over the whole range of temperatures are obtained in general by the PCP-SAFT equation as shown in Table 4; the second best by PC-SAFT, followed by CPA and the worst by PR.

At the lower temperatures, deviations of PR, CPA and PCP-SAFT for pressure are larger and tend to decrease with an increase in temperature. The opposite behaviour can be observed for PC-SAFT, where deviations tend to increase as temperature increases. PR and CPA cannot predict the phase behaviour at 313.1 K, and the best prediction is that given

by PC-SAFT. PR is still unable to predict the 343.2 and 373.1 K isotherms. At these conditions deviations of PC-SAFT and PCP-SAFT for pressure are around half those of CPA, with better predictions given by PC-SAFT. At 423.2 K and above, PR gives some prediction of the phase behaviour, but over-predicts the bubble pressure and vapour compositions as well as experiencing convergence problems near the azeotrope. PC-SAFT cannot capture the azeotropic behaviour; whereas contrary to this, CPA can give at least a qualitative representation (Figures 3 and 4). There is clearly an improvement in the predictions when the dipole moment is accounted for in the model at the highest temperatures, with PCP-SAFT giving the best predictions with errors as low as 3.84% in pressure.

3.2.2.2   *Correlative mode*

Binary interaction parameters for each EoS and temperature, obtained from the fitting procedure described above, are presented in Table 5. PC-SAFT binary parameters are the only ones positive in sign for the EoS studied; their values increase as the temperature increases. In contrast, the binary parameters for PCP-SAFT shift in magnitude from high to lower magnitudes and from negative to positive. Since a temperature dependency was observed, a single temperature-dependent binary interaction parameter with the form k_{ij} k_{ij}^0 $k_{ij}^1 T$ was fitted. Coefficients k_{ij}^0 and k_{ij}^1 are presented in Table 5. Calculated deviations in pressure and compositions for this temperature-dependent k_{ij} are shown in Table 4.

Using a binary interaction parameter, PR is able to give a representation of the phase diagrams at low temperatures, e.g. the 313.1 K isotherm shown in Figure 5. It results in improved correlations and similar magnitudes of the binary parameter when compared with CPA for most temperatures (except at 453.2 and 483.2 K, for which a double value of k_{ij} is required for PR). Correlations of the bubble pressures and compositions, and better representations of the azeotrope are obtained with PCP-SAFT (Figures 6 and 7). PC-SAFT in correlative mode can capture the azeotropic behaviour but it tends to over-predict the corresponding pressure.

Figure 8 shows isobaric data at 1 bar from different literature sources and the modelling with the selected EoS. As depicted, the PCP-SAFT correlation is the closest to the average experimental data. PC-SAFT curves are comparable with those previously reported by Janecek and Paricaud [30] and Chen et al. [21], using a positive binary interaction parameter (k_{ij} 0.03). The largest deviations from the experimental data are encountered with CPA. Even with a large negative value of the binary parameter (0.15), it is not possible to obtain a satisfactory representation of the phase behaviour, particularly of the dew-line. A better approximation (not plotted) is gained through a temperature-dependent (k_{ij} k_{ij}^0 $k_{ij}^1 T$) parameter, but yet still, without satisfactory results. Correlations could be improved by means of a different association scheme as shown by Kontogeorgis et al. [31] who modelled the system considering propanoic acid and water as 1A and 4C, respectively; a k_{ij} 0.21 was however, necessary. In light of the information in Figure 8, PR correlations can be considered satisfactory.

4. Conclusions

New experimental data were determined for the propanoic acid + water system at 423.2, 453.2 and 483.2 K with a static-analytical apparatus. The mixture is highly non-ideal exhibiting positive deviations from Raoults's low with azeotropism. Inclusion of the association and dipolar contributions enhances the capabilities of PC-SAFT in modelling the propanoic acid + water mixtures. PCP-SAFT showed higher predictive and correlative properties over the range of temperatures making it the best option for modelling this system. The second best option is PC-SAFT based on the correlations. From an engineering point of view, CPA could be an adequate modelling tool since it presents a balance between predictive

and correlative properties and is relatively easier to implement than PC-SAFT or PCP-SAFT. For correlation purposes only, PR could be a suitable option.

Acknowledgements

References

[1] PR Newswire Propionic Acid and Derivatives Market Worth $1,622.2 Million by 2018. http://www.prnewswire.com/news-releases/propionic-acid--derivatives-market-worth-16222-million-by-2018-217569611.html (09 August 2014).

[2] Samel, U.-R.; Kohler, W.; Gamer, A. O.; Keuser, U., *Propionic Acid and Derivatives* [online]; Wiley-VCH: 2011; pp. 295-311. http://dx.doi.org/10.1002/14356007.a22_223.pub2 (07 August 2014).

[3] Chiusoli, G. P.; Maitlis, P. M., *Metal-Catalysis in Industrial Organic Processes* [online]; Royal Society of Chemistry: 2006; pp. 119-120. http://app.knovel.com/hotlink/toc/id:kpMCIOP001/metal-catalysis-in-industrial/metal-catalysis-in-industrial (July 2014).

[4] Demirbas, A., Biorefineries: Current Activities and Future Developments. *Energy Convers. Manage.* **2009**, *50*, 2782-2801.

[5] Goodwin, A. K.; Rorrer, G. L., Reaction Rates for Supercritical Water Gasification of Xylose in a Micro-Tubular Reactor. *Chem. Eng. J.* **2010**, *163* (1-2), 10-21.

[6] Giacalone, A.; Accascina, F.; Carnesi, G., Surface Activity VIII. Surface Activity and Vapor Pressure of Aqueous Solutions of Aliphatic Acids. *Gazz. Chim. Ital.* **1942**, *72*, 109.

[7] Othmer, D. F., Composition of Vapors from Boiling Binary Solutions. *Ind. Eng. Chem.* **1943**, *35*, 614-620.

[8] Gmehling, J.; Onken, U., *Vapor–Liquid Equilibrium Data Collection: Aqueous–Organic Systems*. Chemistry Data Series. DECHEMA: Frankfurt, Germany, 1977; Vol. 1. Part 1.

[9] Miyamoto, S.; Nakamura, S.; Iwai, Y.; Arai, Y., Measurement of Isothermal Vapor–Liquid Equilibria for Binary and Ternary Systems Containing Monocarboxylic Acid. *J. Chem. Eng. Data* **2001**, *46* (5), 1225-1230.

[10] Olson, J. D.; Morrison, R. E.; Wilson, L. C., Thermodynamics of Hydrogen-Bonding Mixtures. 5. G^E, H^E, and TS^E and Zeotropy of Water + Acrylic Acid. *Ind. Eng. Chem. Res.* **2008**, *47* (15), 5127-5131.

[11] Leeke, G. A.; Santos, R.; King, M. B., Vapor–Liquid Equilibria for the Carbon Dioxide + Carvacrol System at Elevated Pressures. *J. Chem. Eng. Data* **2001**, *46* (3), 541-545.

[12] Economou, I. G., Cubic and Generalized Van Der Waals Equations of State. In *Applied Thermodynamics of Fluids*, Goodwin, A. R. H.; Sengers, J. V.; Peters, C. J., Eds. Royal Society of Chemistry: 2010.

[13] McCabe, C.; Galindo, A., SAFT Associating Fluids and Fluid Mixtures. In *Applied Thermodynamics of Fluids*, Goodwin, A. R. H.; Sengers, J. V.; Peters, C. J., Eds. Royal Society of Chemistry: 2010.

[14] Kontogeorgis, G. M.; Folas, G. K., *Thermodynamic Models for Industrial Applications*. John Wiley and Sons: West Sussex, United Kingdom, 2010.

[15] Huang, S. H.; Radosz, M., Equation of State for Small, Large, Polydisperse, and Associating Molecules. *Ind. Eng. Chem. Res.* **1990**, *29* (11), 2284-2294.

[16] von Solms, N.; Michelsen, M. L.; Passos, C. P.; Derawi, S. O.; Kontogeorgis, G. M., Investigating Models for Associating Fluids Using Spectroscopy. *Ind. Eng. Chem. Res.* **2006**, *45* (15), 5368-5374.

[17] Kontogeorgis, G. M.; Michelsen, M. L.; Folas, G. K.; Derawi, S.; von Solms, N.; Stenby, E. H., Ten Years with the CPA (Cubic-Plus-Association) Equation of State. Part 1. Pure Compounds and Self-Associating Systems. *Ind. Eng. Chem. Res.* **2006**, *45* (14), 4855-4868.

[18] Aparicio-Martínez, S.; Hall, K. R., Phase Equilibria in Water Containing Binary Systems from Molecular Based Equations of State. *Fluid Phase Equilib.* **2007**, *254* (1-2), 112-125.

[19] Kleiner, M. Thermodynamic Modeling of Complex Systems: Polar and Associating Fluids and Mixtures. Doctoral Dissertation, Dortmund University of Technology, Dortmund, Germany, 2008.

[20] Soo, C. B. Experimental Thermodynamic Measurements of Biofuel-Related Associating Compounds and Modeling Using the PC-SAFT Equation of State. Doctoral Thesis, École Nationale Supérieure des Mines de Paris, Paris, France, 2011.

[21] Chen, Y.; Afef, A.; Fabrice, M.; Roland, S.; Jeday, M. R., Thermodynamic Modeling of Mixtures Containing Carboxylic Acids Using the PC-SAFT Equation of State. *Ind. Eng. Chem. Res.* **2012**, *51* (42), 13846-13852.

[22] Liang, X.; Tsivintzelis, I.; Kontogeorgis, G. M., Modeling Water Containing Systems with the Simplified PC-SAFT and CPA Equations of State. *Ind. Eng. Chem. Res.* **2014**, *53* (37), 14493-14507.

[23] Heisler, I. A.; Mazur, K.; Yamaguchi, S.; Tominaga, K.; Meech, S. R., Measuring Acetic Acid Dimer Modes by Ultrafast Time-Domain Raman Spectroscopy. *PCCP* **2011**, *13* (34), 15573-15579.

[24] Kleiner, M.; Tumakaka, F.; Sadowski, G., Thermodynamic Modeling of Complex Systems. In *Molecular Thermodynamics of Complex Systems*, Lu, X.; Hu, Y., Eds. Springer Berlin Heidelberg: 2009; Vol. 131, pp 75-108.

[25] Derawi, S. O.; Zeuthen, J.; Michelsen, M. L.; Stenby, E. H.; Kontogeorgis, G. M., Application of the CPA Equation of State to Organic Acids. *Fluid Phase Equilib.* **2004**, *225*, 107-113.

[26] Janecek, J.; Paricaud, P., Influence of Cyclic Dimer Formation on the Phase Behavior of Carboxylic Acids. *J. Phys. Chem. B* **2012**, *116* (27), 7874-7882.

[27] Sear, R. P.; Jackson, G., Thermodynamic Perturbation-Theory for Association into Doubly Bonded Dimers. *Mol. Phys.* **1994**, *82* (5), 1033-1048.

[28] Sear, R. P.; Jackson, G., Thermodynamic Perturbation Theory for Association into Chains and Rings. *Phys. Rev. E* **1994**, *50* (1), 386-394.

[29] Kouskoumvekaki, I. A.; Krooshof, G. J. P.; Michelsen, M. L.; Kontogeorgis, G. M., Application of the Simplified PC-SAFT Equation of State to the Vapor–Liquid Equilibria of Binary and Ternary Mixtures of Polyamide 6 with Several Solvents. *Ind. Eng. Chem. Res.* **2004**, *43* (3), 826-834.

[30] Janecek, J.; Paricaud, P., Influence of Cyclic Dimer Formation on the Phase Behavior of Carboxylic Acids. II. Cross-Associating Systems. *J. Phys. Chem. B* **2013**, *117* (32), 9430-9438.

[31] Kontogeorgis, G. M.; Folas, G. K.; Muro-Suñé, N.; von Solms, N.; Michelsen, M. L.; Stenby, E. H., Modelling of Associating Mixtures for Applications in the Oil & Gas and Chemical Industries. *Fluid Phase Equilib.* **2007**, *261* (1-2), 205-211.

[32] Muro-Suné, N.; Kontogeorgis, G. M.; von Solms, N.; Michelsen, M. L., Phase Equilibrium Modelling for Mixtures with Acetic Acid Using an Association Equation of State. *Ind. Eng. Chem. Res.* **2008**, *47* (15), 5660-5668.

[33] Smith, J. W., *Electric Dipole Moments*. Butterworths Scientific Publications: London, 1955; p 370.

[34] Alsaifi, N. M.; Hamad, E. Z.; Englezos, P., Prediction of Vapor–Liquid Equilibrium in Water–Alcohol–Hydrocarbon Systems with the Dipolar Perturbed-Chain SAFT Equation of State. *Fluid Phase Equilib.* **2008**, *271* (1-2), 82-93.

[35] Román-Ramírez, L. A.; García-Sánchez, F.; Ortiz-Estrada, C. H.; Justo-García, D. N., Modeling of Vapor–Liquid Equilibria for CO_2 + 1-Alkanol Binary Systems with the PC-SAFT Equation of State Using Polar Contributions. *Ind. Eng. Chem. Res.* **2010**, *49* (23), 12276-12283.

[36] Kleiner, M.; Sadowski, G., Modeling of Polar Systems Using PCP-SAFT: An Approach to Account for Induced-Association Interactions. *J. Phys. Chem. C* **2007**, *111* (43), 15544-15553.

[37] Garverick, L., *Corrosion in the Petrochemical Industry* [online]; ASM International: 1994; p 186-191. http://app.knovel.com/hotlink/toc/id:kpCPI00002/corrosion-in-petrochemical (January 2013).

[38] NIST. Chemistry Webbook. NIST Standard Reference Database 69. [online]; http://webbook.nist.gov/chemistry/ (October 2012).

[39] Peng, D.-Y.; Robinson, D. B., A New Two-Constant Equation of State. *Ind. Eng. Chem. Fundam.* **1976**, *15* (1), 59-64.

[40] Michelsen, M. L.; Mollerup, J., *Thermodynamic Models: Fundamentals and Computational Aspects*. 2nd ed.; Tie-Line Publications: Denmark, 2007.

[41] Kontogeorgis, G. M.; Voutsas, E. C.; Yakoumis, I. V.; Tassios, D. P., An Equation of State for Associating Fluids. *Ind. Eng. Chem. Res.* **1996**, *35* (11), 4310-4318.

[42] Gross, J.; Vrabec, J., An Equation-of-State Contribution for Polar Components: Dipolar Molecules. *AIChE J.* **2006**, *52* (3), 1194-1204.

[43] Gross, J.; Sadowski, G., Perturbed-Chain SAFT: An Equation of State Based on a Perturbation Theory for Chain Molecules. *Ind. Eng. Chem. Res.* **2001**, *40* (4), 1244-1260.

[44] Gross, J.; Sadowski, G., Application of the Perturbed-Chain SAFT Equation of State to Associating Systems. *Ind. Eng. Chem. Res.* **2002**, *41* (22), 5510-5515.

[45] Othmer, D. F.; Silvis, S. J.; Spiel, A., Composition of Vapors from Boiling Binary Solutions. Pressure Equilibrium Still for Studying Water–Acetic Acid System. *Ind. Eng. Chem.* **1952**, *44* (8), 1864-1872.

[46] Kontogeorgis, G. M.; Tsivintzelis, I.; von Solms, N.; Grenner, A.; Bøgh, D.; Frost, M.; Knage-Rasmussen, A.; Economou, I. G., Use of Monomer Fraction Data in the Parametrization of Association Theories. *Fluid Phase Equilib.* **2010**, *296* (2), 219-229.

[47] Tybjerg, P. C. V.; Kontogeorgis, G. M.; Michelsen, M. L.; Stenby, E. H., Phase Equilibria Modeling of Methanol-Containing Systems with the CPA and sPC-SAFT Equations of State. *Fluid Phase Equilib.* **2010**, *288* (1–2), 128-138.

[48] Karakatsani, E. K.; Economou, I. G., Phase Equilibrium Calculations for Multi-Component Polar Fluid Mixtures with tPC-PSAFT. *Fluid Phase Equilib.* **2007**, *261* (1-2), 265-271.

[49] Brazauskiene, J.; Mishchenko, K. P.; Ciparis, J., The Liquid–Vapor Equilibrium in the Propionic Acid–Water System under Isothermal Conditions (40, 50, 60 °C). *Lietuvos TSR Aukštųjų Mokyklų Mokslo Darbai. Chem. Chem. Technol.* **1965**, *6*.

[50] Rafflenbeul, L.; Hartmann, H., Eine Dynamische Apparatur Zur Bestimmung Von Dampf-Flüssigkeits-Phasengleichgewichten. *Chem. Ing. Tech.* **1978**, *7*.

[51] DIPPR, *801 Database. Data Compilation of Pure Compound Properties.* AIChE: 2012.

[52] Rivenq, F., Vapor–Liquid Data for the System Water–Propionic Acid. *Bull. Soc. Chim. Fr.* **1961**, 1392-1395.

[53] Ito, T.; Yoshida, F., Vapor–Liquid Equilibria of Water–Lower Fatty Acid Systems: Water–Formic Acid, Water–Acetic Acid and Water–Propionic Acid. *J. Chem. Eng. Data* **1963**, *8* (3), 315-320.

[54] Kushner, T. M.; Tatsievskaya, G. I.; Serafimov, L. A., Liquid–Vapor Phase Equilibrium in the Water–Formic Acid–Propionic Acid System under Atmospheric Pressure. *Zh. Fiz. Khim.* **1967**, *41*, 237.

[55] Amer, S., Vapor–Liquid Equilibrium in Binary Systems Formed by Propionic Acid with Water and Amyl Alcohol, Isoamyl Alcohol, Secondary Amyl Alcohol, Tertiary Amyl Alcohol and Hexanol at 760 mmHg. *An. Quim.* **1975**, *71* (2), 127-135.

Figure captions

Figure 1. Association schemes for organic acids and water based on the classification of Huang and Radosz [15].

Figure 2. Schematic drawing of the experimental static-analytical apparatus. EC, equilibrium cell; AB, air bath; DPG, digital pressure gauge; TDL, thermocouple data logger; LSV, liquid sampling valve; VSV, vapour sampling valve; GC, gas-chromatograph; 3WY, three-way valve; VP, vacuum-pump; DLP, digital liquid-pump; RV, relief valve; WS, water supply; MD, magnetic drive.

Figure 3. Vapour – liquid diagram for the propanoic acid (1) + water (2) system at 453.2 K. Experimental data (●) from this work. Lines: equation of state predictions (k_{ij} 0).

Figure 4. Vapour – liquid diagram for the propanoic acid (1) + water (2) system at 483.2 K. Experimental data (●) from this work. Lines: equation of state predictions (k_{ij} 0).

Figure 5. Vapour – liquid diagram for the propanoic acid (1) + water (2) system at 313.1 K. Experimental data (●) from Brazauskiene et al. [49]. Lines: equation of state correlations (k_{ij} k_{ij}^0 $k_{ij}^1 T$).

Figure 6. Vapour – liquid diagram for the propanoic acid (1) + water (2) system at 373.1 K. Experimental data (●) from Rafflenbeul and Hartmann [50]. Lines: equation of state correlations (k_{ij} k_{ij}^0 $k_{ij}^1 T$).

Figure 7. Vapour – liquid diagram for the propanoic acid (1) + water (2) system at 423.2 K. Experimental data (●) from this work. Lines: equation of state correlations (k_{ij} k_{ij}^0 $k_{ij}^1 T$).

Figure 8. Vapour – liquid diagram for the propanoic acid (1) + water (2) system at 1 bar. Experimental data: (■), Rivenq [52]; (▲), Ito and Yoshida [53]; (x), Kushner et al. [54] and (●), Amer [55]. Lines: equation of state correlations.

Table 1. Experimental vapour – liquid equilibrium data for propanoic acid (1) + water (2) system at pressure P, liquid mole fraction x, vapour mole fraction y and temperatures $T = 423.2$, 453.2 and 483.2 K. Combined standard uncertainties, u_c, are u_c T $= 0.1$ K, $u_c(P) = 0.01$ bar. $u_c(x)$ and $u_c(y)$ are displayed in each temperature column.

$T = 423.2$ K					$T = 453.2$ K					$T = 483.2$ K				
P / bar	x_1	y_1	$u_c(x_1)$	$u_c(y_1)$	P / bar	x_1	y_1	$u_c(x_1)$	$u_c(y_1)$	P / bar	x_1	y_1	$u_c(x_1)$	$u_c(y_1)$
1.87	0.973	0.705	0.005	0.005	4.15	0.960	0.701	0.005	0.005	7.94	0.946	0.647	0.003	0.023
2.34	0.932	0.498	0.005	0.005	5.04	0.918	0.512	0.003	0.005	10.00	0.880	0.393	0.006	0.022
2.74	0.881	0.406	0.005	0.005	6.02	0.850	0.340	0.007	0.013	11.64	0.817	0.271	0.005	0.033
3.26	0.809	0.285	0.004	0.003	6.83	0.774	0.252	0.005	0.005	13.06	0.760	0.204	0.003	0.013
3.77	0.675	0.231	0.008	0.018	7.36	0.724	0.204	0.003	0.004	14.16	0.708	0.152	0.011	0.018
4.11	0.550	0.200	0.005	0.021	8.23	0.600	0.155	0.005	0.005	15.23	0.643	0.119	0.016	0.012
4.31	0.477	0.159	0.004	0.012	8.92	0.482	0.128	0.015	0.005	16.48	0.534	0.105	0.005	0.005
4.56	0.366	0.137	0.005	0.005	9.36	0.398	0.116	0.005	0.005	17.04	0.479	0.098	0.005	0.005
4.60	0.344	0.123	0.003	0.003	9.84	0.292	0.108	0.005	0.005	17.65	0.413	0.094	0.005	0.005
4.70	0.281	0.104	0.005	0.005	10.00	0.226	0.102	0.005	0.005	18.25	0.339	0.090	0.005	0.005
4.75	0.225	0.100	0.005	0.005	10.07	0.169	0.092	0.005	0.005	18.91	0.233	0.086	0.005	0.005
4.78	0.145	0.096	0.005	0.005	10.08	0.160	0.090	0.005	0.005	19.10	0.184	0.081	0.005	0.005
4.80	0.130	0.086	0.005	0.005	10.10	0.133	0.079	0.005	0.005	19.35	0.128	0.072	0.005	0.005
4.82	0.111	0.084	0.005	0.005	10.05	0.017	0.027	0.005	0.005	19.38	0.105	0.069	0.005	0.005
4.81	0.074	0.071	0.005	0.005	10.03	0.000	0.000			19.35	0.017	0.024	0.005	0.005
4.80	0.017	0.026	0.005	0.005						19.02	0.000	0.000		
4.76	0.000	0.000												

Table 2. Pure component properties.[a]

Compound	$M/$g/gmol	$Pc/$bar	Tc / K	ω
propanoic acid	74.08	46.68	600.81	0.580
water	18.02	220.64	647.10	0.345

[a] Molar mass (M), critical pressure (P_c), critical temperature (T_c) and acentric factor (ω). Data from DIPPR database [51].

Table 3. CPA, PC-SAFT and PCP-SAFT pure component parameters and average deviations in vapour pressures (P_v) and liquid densities (ρ_L).[a,b]

CPA

Compound	$a_0 / \text{bar L}^2 \text{mol}$	$b / \text{L mol}^{-1}$	c_1	ε^{AB}/K	β^{AB}	T/K	$P_V / \%$	$\rho_L / \%$	
propanoicacid	9.4034	0.0635	1.0730	2695.9	0.0588	252 - 594	0.47	0.66	
water	2.5108	0.0150	1.0049	1817.6	0.2882	273 - 640	0.81	1.66	

PC-SAFT/PCP-SAFT

Compound	m	$\sigma / \text{Å}$	$\varepsilon/k / K$	k^{AB}	$\varepsilon^{AB}/k / K$	μ / D	T / K	$P_V / \%$	$\rho_L / \%$
	3.2579	3.1047	192.67	0.192751	2647.5			0.55	0.40
propanoic acid	3.1508	3.1436	192.01	0.179171	2664.4	1.751	252 - 594	0.52	0.40
	2.7028	2.0526	218.96	0.561417	2045.0			0.61	2.01
water	2.6206	2.1120	211.82	0.635842	1394.5	1.85	273-640	0.58	1.74

[a] Vapour pressure, liquid density and dipolar moment (μ) data from DIPPR [51].

[b] Two association sites assumed for all substances.

Table 1. PR, CPA, PC-SAFT and PCP-SAFT average deviations in pressure (ΔP) and propanoic acid vapour composition (Δy_1), in predictive mode ($k_{ij} = 0$) and correlative mode ($k_{ij} = k_{ij}^0 + k_{ij}^1 T$). Empty cells: Predictions were not possible.

| | | $k_{ij} = 0$ | | | | | | | | $k_{ij} = k_{ij}^0 + k_{ij}^1 T$ | | | | | | | |
| | | PR | | CPA | | PC-SAFT | | PCP-SAFT | | PR | | CPA | | PC-SAFT | | PCP-SAFT | |
T / K	Ref.	ΔP / %	Δy_1	ΔP / %	Δy_1	ΔP / %	Δy_1	ΔP / %	Δy_1	ΔP / %	Δy_1	ΔP / %	Δy_1	ΔP / %	Δy_1	ΔP / %	Δy_1
313.1	[49]	-	-	-	-	7.48	0.02	26.77	0.11	9.35	0.06	10.71	0.03	7.80	0.03	2.27	0.02
343.2	[9]	-	-	39.43	0.16	15.93	0.04	14.71	0.09	12.41	0.06	14.01	0.06	10.29	0.04	7.62	0.02
373.1	[50]	-	-	26.05	0.11	12.74	0.02	17.52	0.08	6.48	0.05	9.35	0.04	4.89	0.03	2.77	0.04
423.2	This work	35.09	0.09	16.39	0.07	16.59	0.08	7.88	0.05	9.84	0.06	11.28	0.07	8.20	0.06	5.20	0.05
453.2	This work	23.35	0.08	12.35	0.10	17.21	0.12	5.75	0.08	9.48	0.09	10.93	0.10	7.90	0.09	5.11	0.09
483.2	This work	15.72	0.13	9.13	0.15	17.10	0.16	3.84	0.13	7.98	0.13	9.03	0.15	6.29	0.14	3.84	0.13

Table 2. Table 5 PR, CPA, PC-SAFT and PCP-SAFT binary interaction parameters (k_{ii}) for each isotherm, and parameters k_{ii}^0 and k_{ij}^1 in k_{ij} k_{ij}^0 $k_{ij}^1 T$ [a] for the propanoic acid (i) + water (j) system.

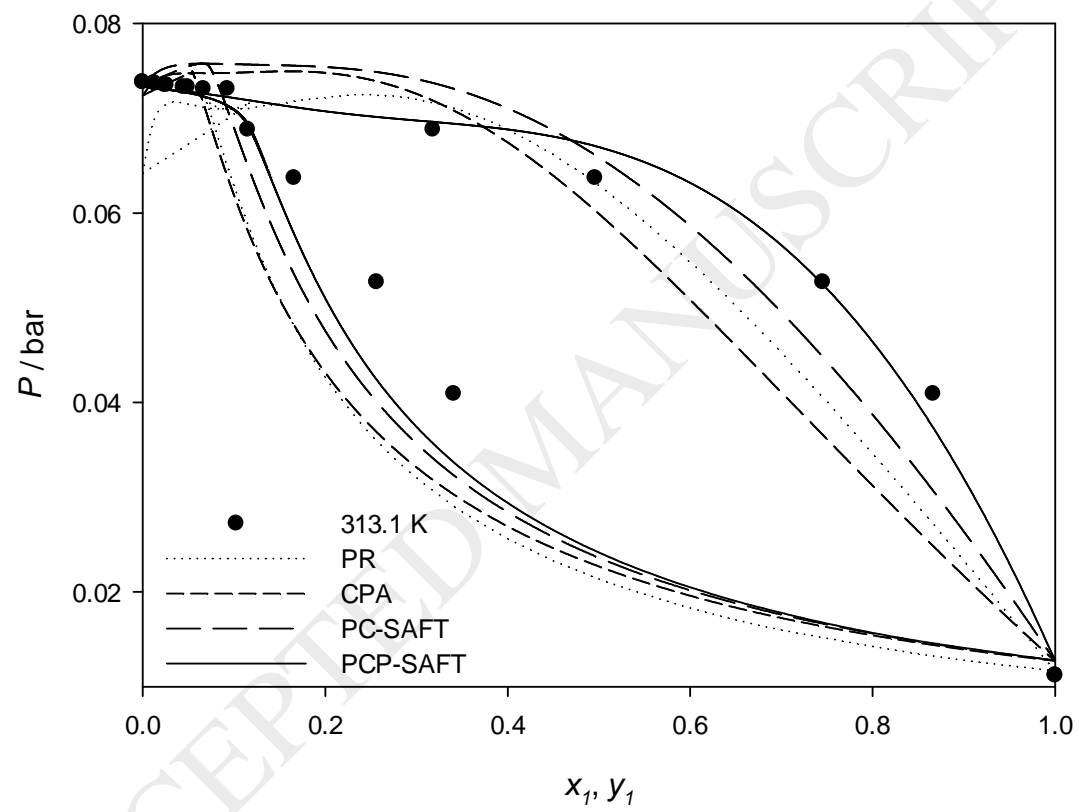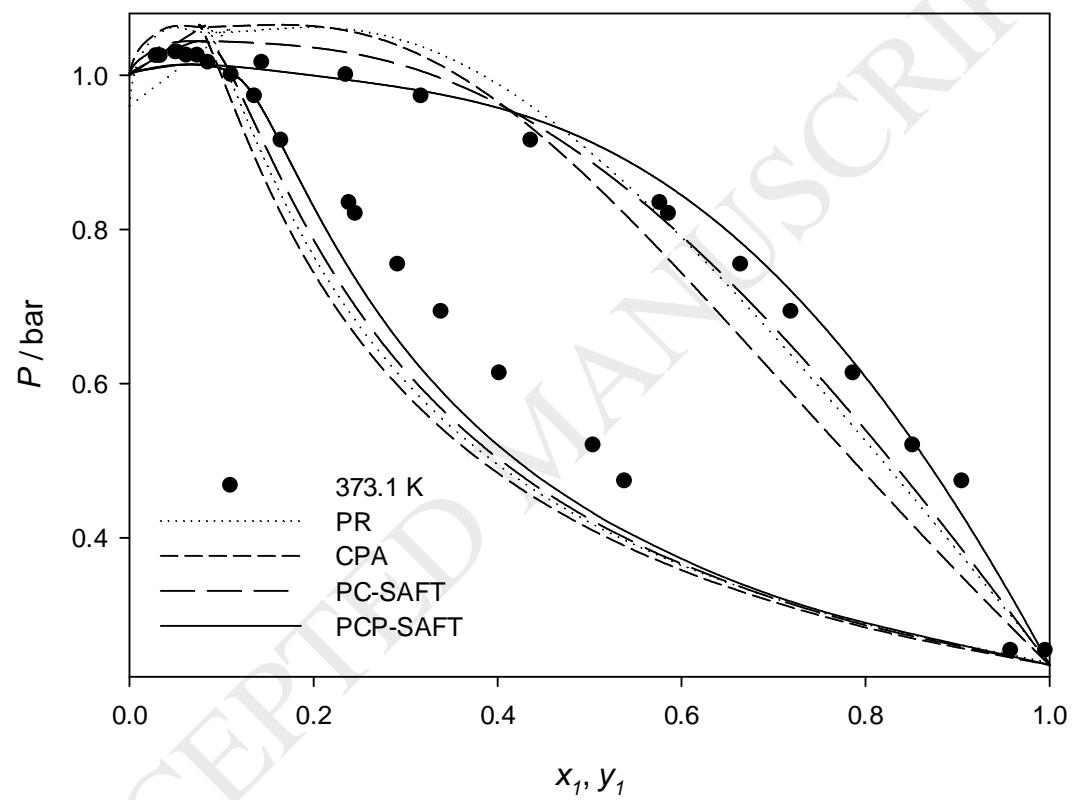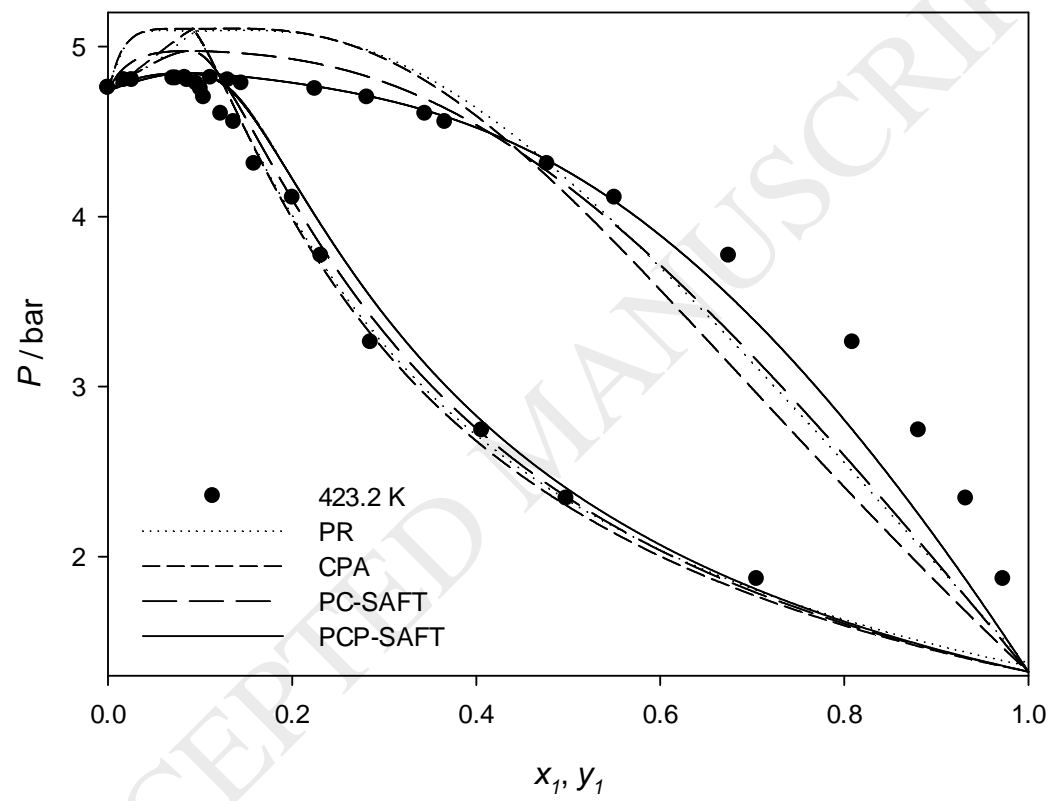| T/ K	Ref.	k_{ij}			
		PR	CPA	PC-SAFT	PCP-SAFT
313.1	[49]	-0.140	-0.182	0.005	-0.062
343.2	[9]	-0.129	-0.147	0.028	-0.045
373.1	[50]	-0.136	-0.134	0.035	-0.046
423.2	This work	-0.118	-0.096	0.045	-0.022
453.2	This work	-0.098	-0.045	0.060	-0.014
483.2	This work	-0.079	-0.010	0.072	0.005
k_{ij}^0		-0.25	-0.49	-0.10	-0.18
$k_{ij}^1 \times 10^4$		3.36	9.72	3.54	3.68

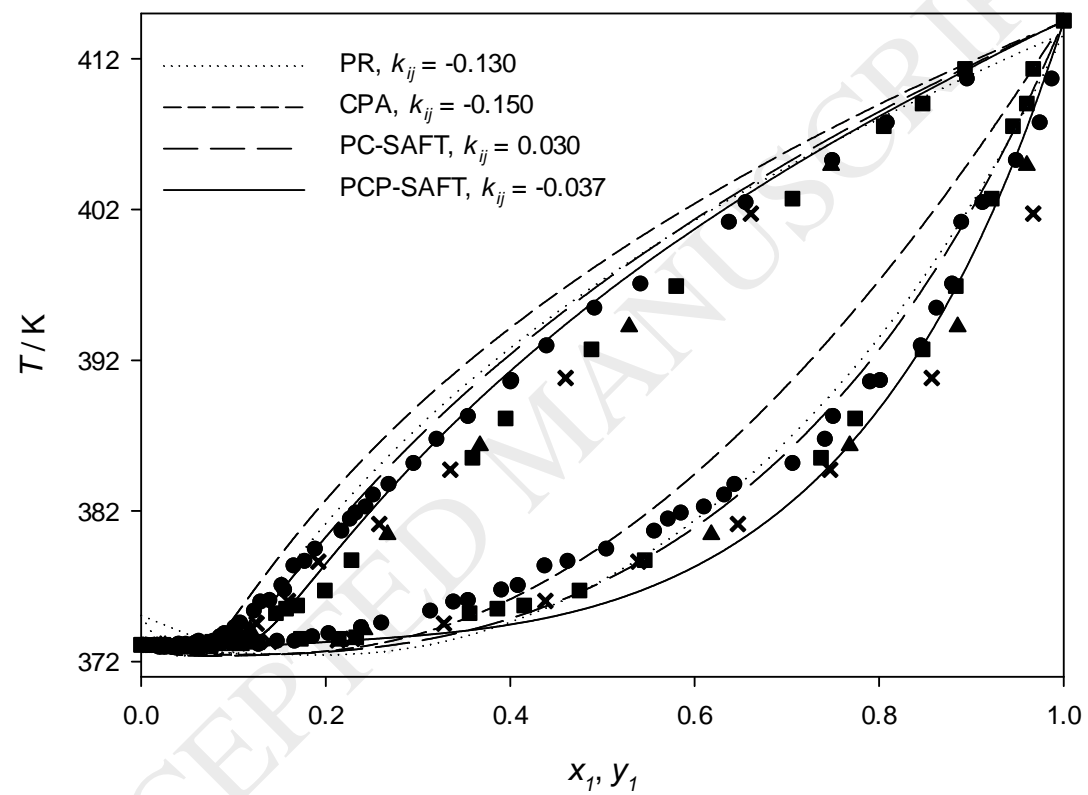[a]Temperature, T, in K.
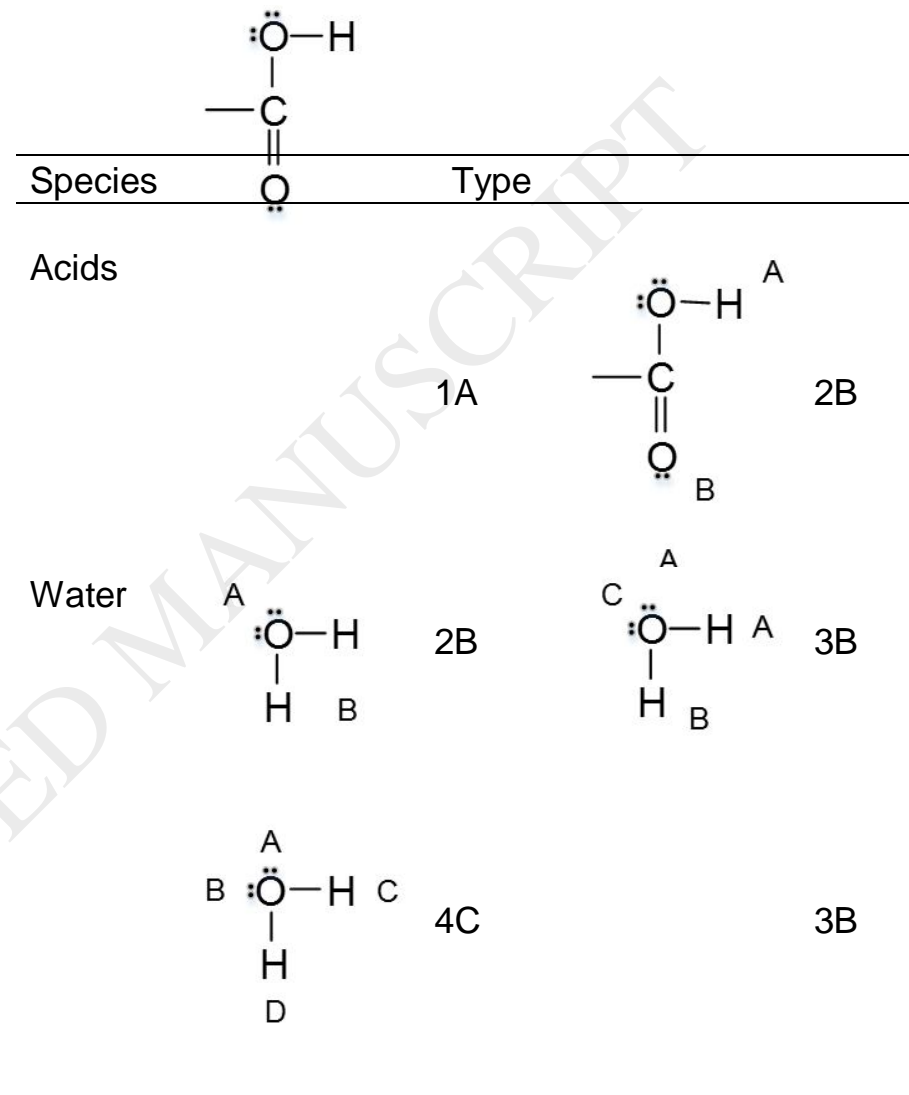
Figure 1.
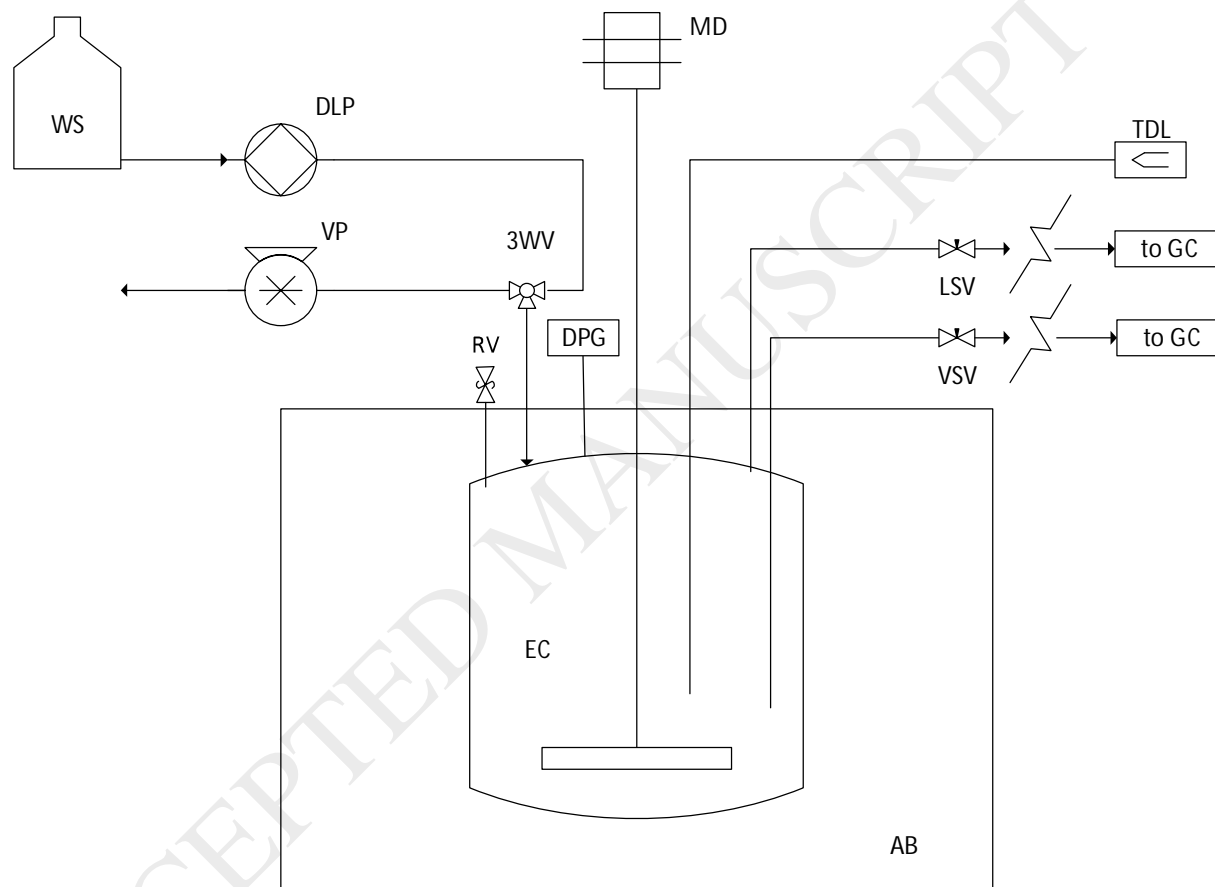
Figure 2.
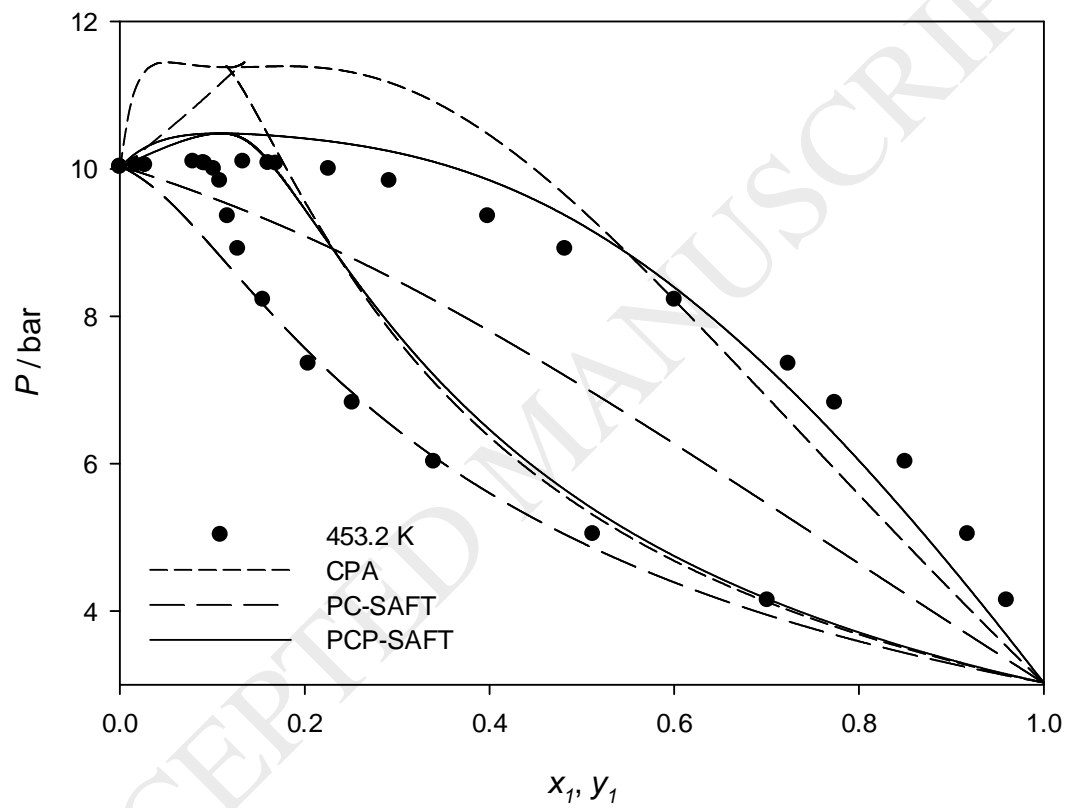
Figure 3
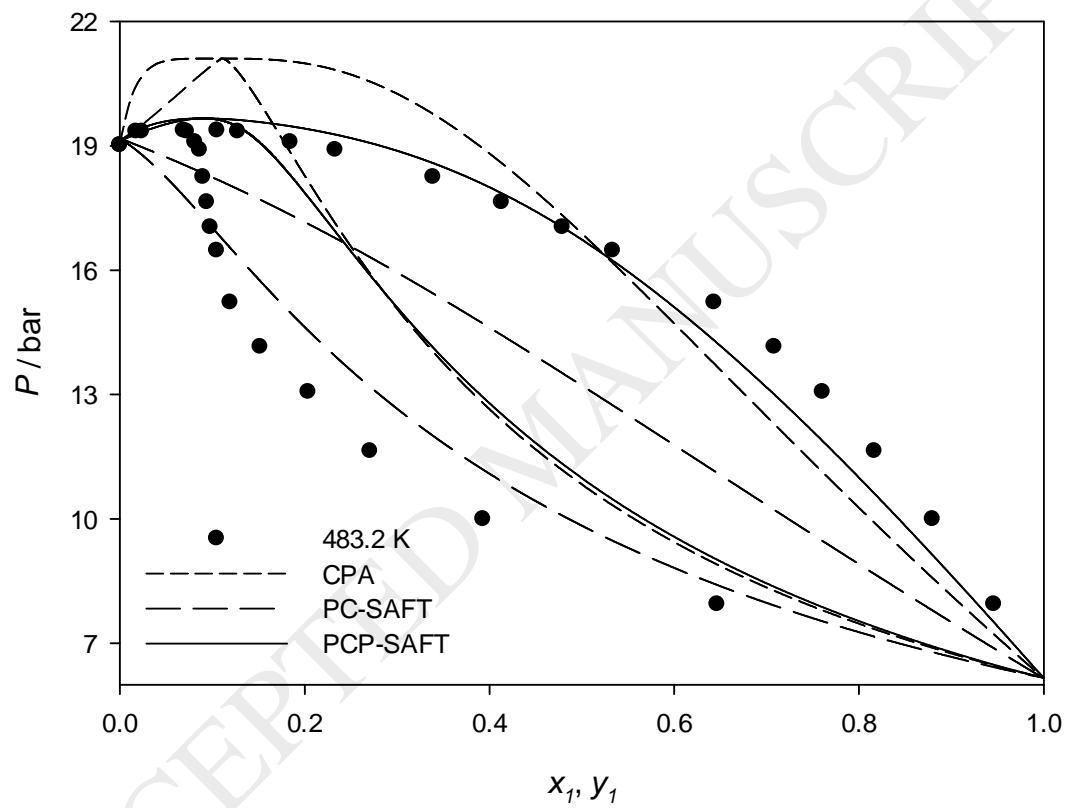
Figure 4

Figure 5.

Figure 6.

Figure 7.

Figure 8